Design of Direct Torque Controller of Induction Motor (DTC)

ALNASIR, Z.A.
Dept. of Electrical and computer Engineering
University of Waterloo N2L 3G1
CANADA
Email: buyazen@hotmail.com

ALMARHOON A.H.
Dept. of Electrical and Electronic Engineering
Jubail Industrial College 10099
Saudi Arabia 31961
Email: marhoon16@hotmail.com

Abstract-

Induction motors are currently used in many industrial applications. Thus, their control techniques have received a lot of interest. An efficient method of induction motor control is the direct torque control (DTC). In this project, a DTC model has been developed and tested using a MATLAB/SIMULINK package. A 6 kW three phase induction motor has been used in order to run and evaluate the developed model. Simulation results have shown the validity and high accuracy of the proposed model. The independence of torque and stator flux control has been confirmed. However, further work should be done in order to limit the significant variation in the starting up stator current caused by any small variation in the stator flux in the developed DTC model.

***Index Terms*….Induction motor, state feedback and estimator.**

I. LIST OF SYMBOLS

IM	Induction motor
DTC	Direct torque control
VC	Vector Control
Hz	Hertz
Ω	Ohm
IM	Induction motor
DTC	Direct Torque Control
Rad/s	Radian per second
MMF	magnetic omotive Force
Wb	Weber
kW	Kilo-Watt
Nm	Newtown-meter
PWM	Pulse Width Modulation
e	Excitation reference frame
VSI	Voltage source inverter
P	Number of pair of poles
Te	Electromagnetic Torque
R	Resistance
L	Inductance
J	Inertia
ω_s	Stator angular speed
ω_r	Rotor angular speed
s	Slip
ψ	Flux linkage
dq	Direct and quadrature axes
LTI	Linear time invariant

II. INTRODUCTION

Because of their robustness, cheapness, high speed operation and less maintenance requirements, the induction motors (IM) are the most common type of electromechanical drive in industrial, commercial and residential applications. To reach the best efficiency of induction motor drive (IMD), many new techniques of control have been developed in the last few years.

In general, induction motor can be controlled by both open and closed loop control techniques. These are also known as scalar and vector control (VC) schemes. VC aims to control the rotor flux and torque of the motor by estimating the speed and voltage. This estimation can be either directly done through measurements or indirectly through calculations [1].

A simpler alternative to the vector control is the direct torque control (DTC). While DTC and VC have different concept of operation, they both provide an effective control of the flux and torque.

The direct torque control (DTC) is the main interest of this project and it will be described in the following sections. However, a brief introduction about IM design and characteristics, IM model and its observailbilty and controllability need to be labelled first for better understanding of the project.

III. DESIGN AND OPERATION OF IM

The induction motor (IM) is an alternating current machine having the armature winding on the stator and the field winding on the rotor (See Fig.1).

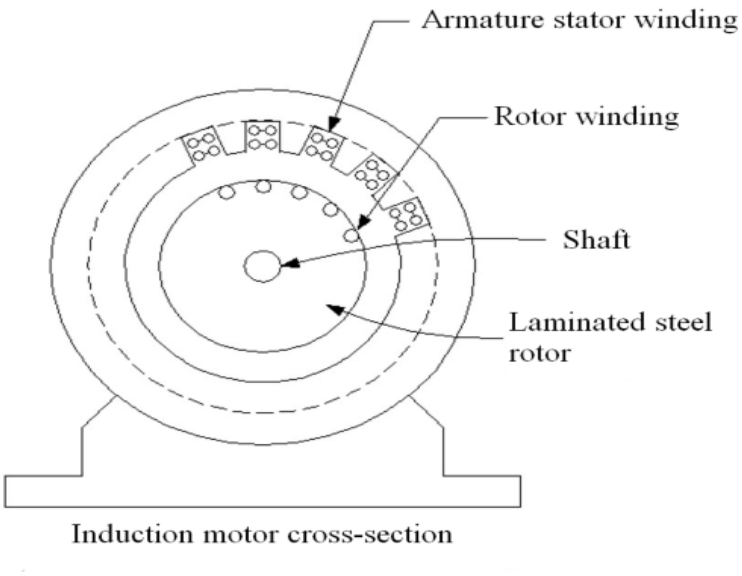

Fig.1. Induction motor cross-section.

When a three phase voltage is applied to the stator winding terminals, three phase balanced currents flow in the armature windings and consequently a rotating magnetic motive force (MMF) field is yielded .This field rotates at synchronous speed (N_s) in revolution per minute.

$N_s = \frac{120\,f}{P}$ where
f : Supply frequency and
P : Number of poles.

By faraday's law, this rotating stator magnetic field induces voltages in the rotor windings causing balanced currents to flow in the short circuited rotor. As a result, a rotor MMF is formed. An electromagnetic torque (Te) is produced due to the interaction between the stator and rotor rotating magnetic fields. The difference between the rotor speed and the stator speed (synchronous speed) defines the per unit slip (s) where

$s = \frac{\omega_s - \omega_r}{\omega_s}$ where
ω_s: Synchronous speed in radian per second and
ω_r : Rotor shaft speed in radian per second.

At zero rotor speed (relaxed condition), a unity slip is produced. At synchronous rotor speed, a nil slip is obtained and hence no torque is produced. The motoring operation of IM is typically in the region of $0 < s < 1$. A typical torque-speed characteristic of an induction motor is shown in Fig.2.

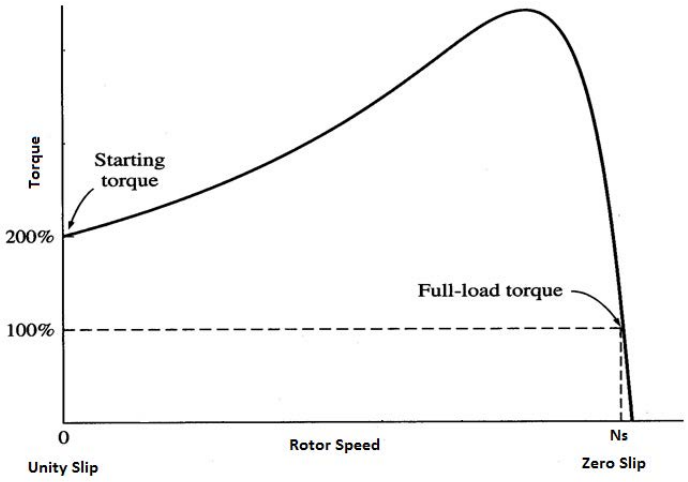

Fig.2. Typical torque-speed characteristic of IM.

The rotor of the induction machine can be either a wound rotor containing three windings similar to the stator once or a squirrel-cage rotor consisting of conducting bars shaped like a squirrel cage.

IV. MODELING ASSUMPTIONS OF IM

In order to design a mathematical model for IM, the following assumptions should be valid.

1- The stator and rotor windings are represented by stator and rotor resistances (R_s , R_r) respectively.

2- The flux in the stator and rotor are represented by stator and rotor inductances (L_s, L_r) respectively.

3- The interaction between stator and rotor fluxes are represented by mutual inductance (L_m).

4- The air gap between stator and rotor is uniformly distributed and hence stator and rotor windings are in sinusoidal distribution.

5- The motor is running at steady state constant speed. (i.e . $\frac{d}{dt}\omega_r = 0$).

6- The motor is initially relaxed.

The IM may be modelled with respect to its stator, its rotor or its synchronous speed. These are known as referencing frames. All variables such as voltage, current and flux in the motor should be referred to the selected frame for modelling. In other words, IM can be modelled in different ways depending on the reference frame selected. In this project, a synchronous frame is taken as a reference for modelling. It makes it easier to apply a direct control as all variables are seen constant with respect to the synchronous frame. The synchronous frame is also called excitation frame subscribed by **e** notation. From now on, any e subscription, unless specified, indicates for synchronous or excitation reference frame. IM models at stator and rotor frames are explained in details in [2].

IM stator current is formulated as a vector with its real element in direct axis (d-axis) and its imaginary element in quadrature axis (q-axis). The d-axis current is used to control the rotor flux while the output torque is controlled by the q-axis current. In other words, flux and torque are independently controlled. Fig.3 illustrates the dq axis and the expressions of current and voltage in that axis.

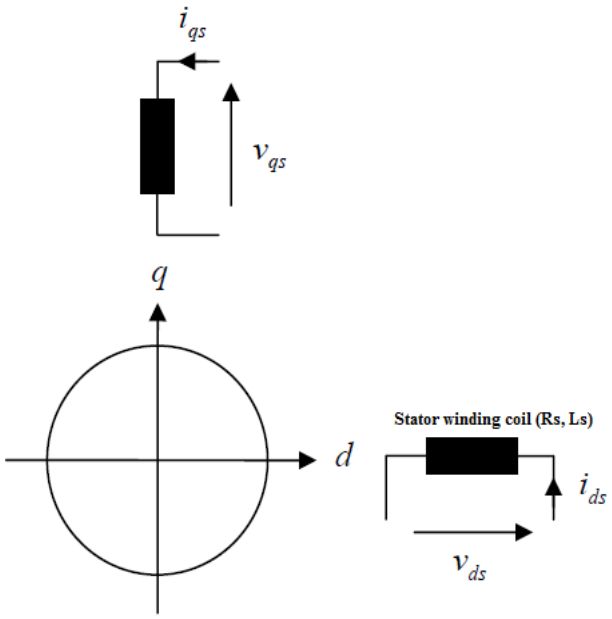

Fig.3. The d-q axes in the stator.

Transformation of the stator current from stator frame to e frame is illustrated in Fig.4 where i_{ds}^{s} , i_{qs}^{s} , i_{ds}^{e} & i_{qs}^{e} are d-axis and q-axis stator currents in stator frame and e frame respectively.

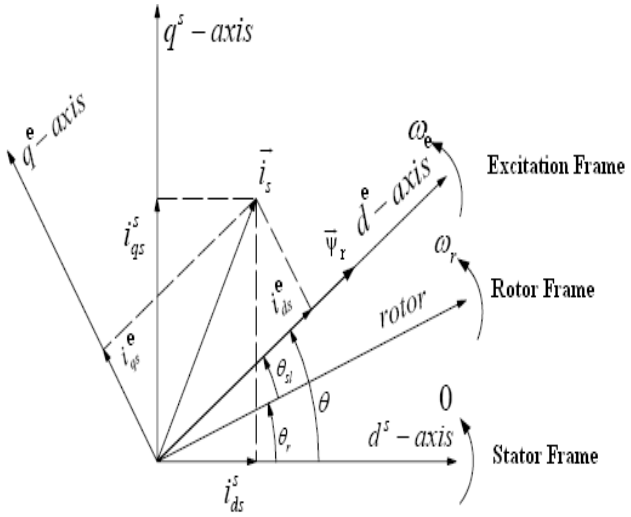

Fig.4. Transformation of stator current vector.

V. STATE SPACE MODEL

The dynamic behaviour of IM is complicated because of mutual coupling between its stator and rotor. Therefore, it is more frequent to use space phasor quantities for induction motor analysis. [3] has illustrated d-q equivalent circuit of an IM as shown in Fig.5.

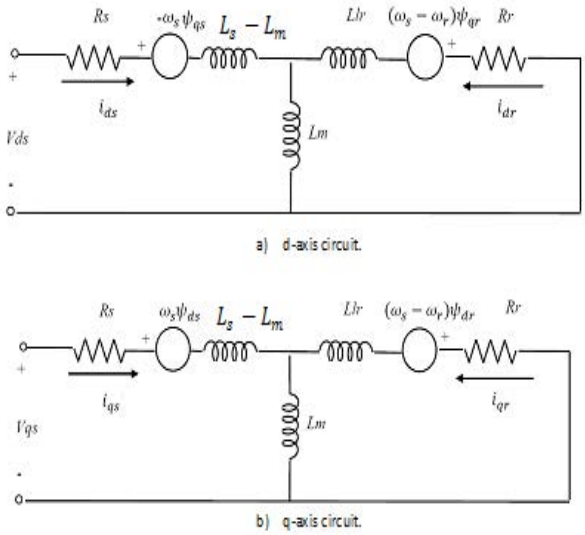

Fig.5. d-q equivalent circuits of IM [3].

The quantities of the d-q equivalent circuits are as follows.

R_s, R_r, L_s, L_r, L_m: as defined in section IV.

ψ_{ds}, ψ_{qs}: d-axis and q-axis stator flux respectively,

ψ_{dr}, ψ_{qr}: d-axis and q-axis rotor flux respectively,

i_{ds}, i_{qs}: d-axis and q-axis stator current respectively,

i_{dr}, i_{qr}: d-axis and q-axis rotor current respectively,

V_{ds}, V_{qs}: d-axis and q-axis stator voltage respectively,

These two circuits may be described in state space format as a linear time invariant (LTI) system.

$$\dot{X} = AX + BU \qquad (1)$$

Assuming zero initial motor speed, the states variables and A , B matrices are as follows.

$$X = \begin{bmatrix} i_{qs} \\ i_{ds} \\ i_{qr} \\ i_{dr} \end{bmatrix}, \quad U = \begin{bmatrix} V_{qs} \\ V_{ds} \\ 0 \\ 0 \end{bmatrix}$$

$$B = \frac{1}{K}\begin{bmatrix} L_r & 0 & -L_m & 0 \\ 0 & L_r & 0 & -L_m \\ -L_m & 0 & L_s & 0 \\ 0 & -L_m & 0 & L_s \end{bmatrix}, \qquad K = L_s L_r - L_m^2$$

$A =$

$$\frac{1}{K}\begin{bmatrix} Rs\,Lr & \omega_s Ls\,Lr - \omega_r L_m^2 & -Rr\,Lm & 0 \\ \omega_r L_m^2 - \omega_s Ls\,Lr & Rs\,Lr & 0 & -Rr\,Lm \\ -Rs\,Lm & 0 & Rr\,Ls & \omega_r Ls\,Lr - \omega_s L_m^2 \\ 0 & -Rs\,Lm & \omega_s L_m^2 - \omega_r Ls\,Lr & RrLs \end{bmatrix}$$

(2)

Another set of equations including the stator and rotor fluxes are required for DTC. The stator flux and the torque are the state variables which need to be estimated and controlled in DTC as will be seen later. Flux equations can be derived from the d-q circuits based on the relation between flux and inductance. (i.e. $\psi = Li$).

$$\frac{d}{dt}\psi_{ds} = -R_s\, i_{ds} + \omega_s \psi_{qs} + V_{ds} \quad (3)$$

$$\frac{d}{dt}\psi_{qs} = -R_s\, i_{qs} - \omega_s \psi_{ds} + V_{qs} \quad (4)$$

$$\frac{d}{dt}\psi_{dr} = -R_r\, i_{dr} + (\omega_s - \omega_r)\psi_{qr} \quad (5)$$

$$\frac{d}{dt}\psi_{qr} = -R_r\, i_{qr} - (\omega_s - \omega_r)\psi_{dr} \quad (6)$$

Equations (3)–(6) are used to estimate the flux and torque based on the observed currents and the control voltage inputs. By applying circuit analysis to Fig.5, the fluxes can be computed as follows.

$$\psi_{ds} = L_{is}\, i_{ds} + L_m\,(i_{ds} + i_{dr}) = L_s\, i_{ds} + L_m\, i_{dr} \quad (7)$$

$$\psi_{dr} = L_{ir}\, i_{dr} + L_m\,(i_{ds} + i_{dr}) = L_r\, i_{dr} + L_m\, i_{ds} \quad (8)$$

$$\psi_{dm} = L_m\,(i_{ds} + i_{dr}) \quad (9)$$

$$\psi_{qs} = L_{is}\, i_{qr} + L_m\left(i_{qs} + i_{qr}\right) = L_s\, i_{qs} + L_m\, i_{qr} \quad (10)$$

$$\psi_{qr} = L_{ir}\, i_{qr} + L_m\left(i_{qs} + i_{qr}\right) = L_r\, i_{qr} + L_m\, i_{qr} \quad (11)$$

$$\psi_{qm} = L_m\left(i_{qs} + i_{qr}\right) \quad (12)$$

By implementing these formulas, Fig.6 shows an induction motor Simulink model developed by the control and drive group in the Electrical, Electronic and Computer Engineering department at Newcastle University (England). This model is being made available as a test case.

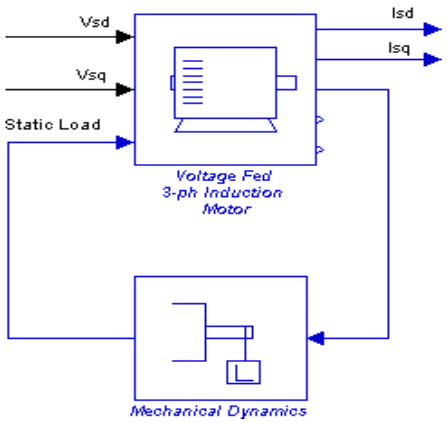

Fig.6. d-q induction motor model.

From Fig.6, it can be noticed that the stator voltages are used as the control input since the rotor is shorted. The stator currents are the output of the model and hence the state space equation of the output can be written as below.

$Y = CX$ Where $C = [1\ \ 1\ \ 0\ \ 0]$.

VI. OBSERVABILITY, CONTROLLABILITY AND STABILITY OF THE IM MODEL

Using the matrices A, B and C, it can be easily shown that both controllability and obesrvability matrices have full rank. In other words,

$\det [B \quad AB \quad A^2B \quad A^3B] \neq 0$

$\det [C \quad CA \quad CA^2 \quad CA^3]^T \neq 0$

Therefore, the IM model is observable and controllable.

Same approach has been used in [2] to show the observability and controllability for the different models with respect to different frames.

By inspection of the state space model, it can be proved that matrix A has a negative real eigenvalue and hence the system is asymptotically stable and bounded input bounded output BIBO stable.

VII. DTC BLOCK DIAGRAM

DTC was introduced by Takahashi (1984) in Japan and then in Germany by Depenbrock (1985) [4]. Unlike the traditional vector control, DTC doesn't require coordinate transformation, PI regulators, PWM and position encoders. Hence, DTC is much simpler. Moreover, Both DTC and VC provide good dynamic response but DTC is less sensitive to the motor parameter variations [5].

DTC Block diagram is shown in Fig.7.Basically, both torque and stator flux need to be estimated so that they can be directly controlled in a way that keeps them within a hysteresis band close to the desired values. This is achieved by choosing the appropriate sector in space vector modulation which will be described in section X. According to [6], the torque produced by a P pole machine can be calculated by equation (13).

$$T_e = \frac{3}{2}\frac{P}{2}\frac{L_m}{L_s L_r}|\psi_r||\psi_s| \sin\theta_{rs} \qquad (13)$$

One can notice that the torque is dependent on the stator flux (ψ_s), rotor flux (ψ_r) and the angle between their vectors (θ_{rs}). However, they will be independently controlled as will be shown in section IX.

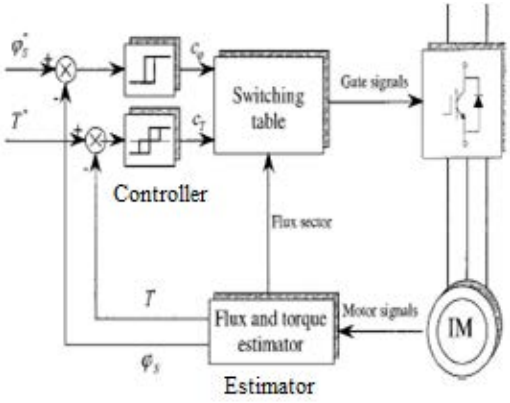

Fig.7. Direct torque control of IM [4].

VIII. ESTIMATOR DESIGN

Considering the d-q axis format shown in Fig.3 earlier, the voltage across the stator coil can be expressed in e frame as follows.

$$\vec{V}_{ds}^{e} = R_s\vec{i}_{ds}^{e} + L_s\frac{d\,\vec{i}_{ds}^{e}}{dt} \qquad (14)$$

$$\vec{V}_{qs}^{e} = R_s\vec{i}_{qs}^{e} + L_s\frac{d\,\vec{i}_{qs}^{e}}{dt} \qquad (15)$$

But,

The term $L_s\frac{d\,\vec{i}_{ds}^{e}}{dt}$ represents the change in stator flux in d and q axis respectively. Hence, (14) & (15) can be reformulated as in (16) & (17) respectively.

$$\vec{V}_{ds}^{e} = R_s \vec{i}_{ds}^{e} + \frac{d\,\vec{\psi}_{ds}^{e}}{dt} \qquad (16)$$

$$\vec{V}_{qs}^{e} = R_s \vec{i}_{qs}^{e} + \frac{d\,\vec{\psi}_{qs}^{e}}{dt} \qquad (17)$$

Solving (16) & (17) for ($\vec{\psi}_{ds}^{e}$& $\vec{\psi}_{qs}^{e}$) yields the following formulas.

$$\vec{\psi}_{ds}^{e} = \int (\vec{V}_{ds}^{e} - R_s \vec{i}_{ds}^{e}) dt \qquad (18)$$

$$\vec{\psi}_{qs}^{e} = \int (\vec{V}_{qs}^{e} - R_s \vec{i}_{qs}^{e}) dt \qquad (19)$$

This means that the stator flux can be estimated as long as the stator current is observable which has been shown earlier. Once the d-q stator currents are known, the stator flux vector and the electromagnetic torque are obtained by (20) & (21).

$$\vec{\psi}_{s}^{e} = \vec{\psi}_{ds}^{e} + j\vec{\psi}_{qs}^{e} \qquad (20)$$

$$T_e = \frac{3}{2} P\,(i_{qs}^{e}\ \psi_{ds}^{e} - i_{ds}^{e}\,\psi_{qs}^{e}) \qquad (21)$$

Where

$\vec{V}_{ds}^{e}$, $\vec{V}_{qs}^{e}$: Stator d-q voltage in e-frame respectively,

$\vec{i}_{ds}^{e}$, $\vec{i}_{qs}^{e}$: Stator d-q current in e-frame respectively,

$\vec{\psi}_{ds}^{e}$, $\vec{\psi}_{qs}^{e}$: Stator d-q flux in e-frame respectively,

T_e , P : Electromagnetic torque and Pole pairs.

Based on the formulas mentioned above, a Simulink models for flux and Torque estimators have been designed as shown in Fig.8.

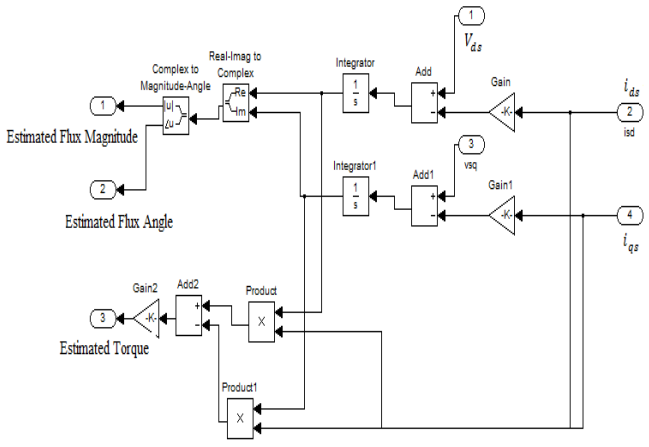

Fig.8. Simulink model of flux and torque estimators.

IX. STATE FEEDBACK DESIGN

The estimated stator flux and torque are to be separately controlled.

A- Flux Controller

The stator flux ($\Delta\vec{\psi}_s$) varies due to the applied stator voltage vector ($\vec{V}_s$) during an interval of time (Δt).

i.e $\Delta\vec{\psi}_s = \vec{V}_s\,\Delta t$ (22)

Therefore, the stator flux is controllable if a proper selection of the voltage vector is made. According to [7], Fig.9 shows that the stator flux plane is divided into six sectors where each one has a set of voltage vectors. Bold arrow indicates the decreasing of the stator flux while the light arrow indicates the increment.

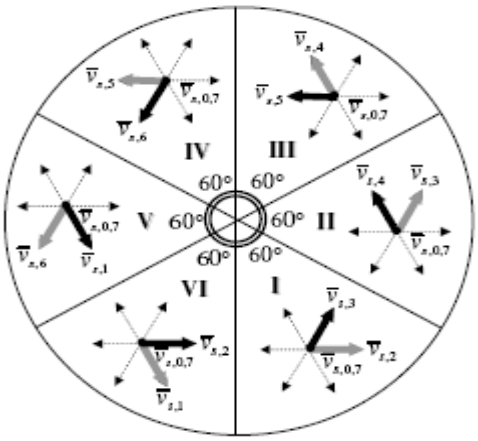

Fig.9. Six sectors with different set of voltages [7].

The estimated stator flux is decreased or increased in order to match the manner of the desired or reference stator flux. However, a hysteresis band should be allowed and hence a 2–level hysteresis comparator is used for accurate design. The flux controller is shown in Fig.10. The flux error which is due to the difference between the estimated and desired stator flux is fed to the hysteresis comparator which in turn produces the flux error status.

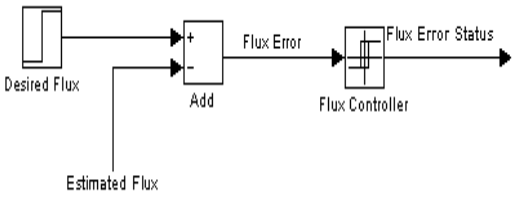

Fig.10. Design of flux controller.

B- Torque Controller

In previous work [4], it has been proved that the instantaneous electromagnetic torque is a sinusoidal function of the angle between the stator and rotor fluxes abbreviated as $\vec{\psi}_s$ & $\vec{\psi}_r$ respectively. The relation between these two flux vectors can be illustrated by Fig.11 where the angle between them is denoted by θ_{sr}.

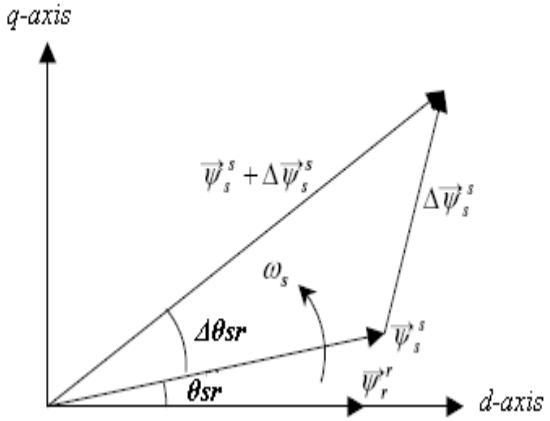

Fig .11. Space vectors of stator and rotor fluxes.

It can be observed that when the stator flux changes quickly, θ_{sr} will be greatly varied causing a high variation in the output torque. Therefore, the inverter voltage vectors must be properly selected in order to obtain a faster speed of so that a good dynamic performance is achieved.

Similar to the flux control, torque is controlled within its 3-level hysteresis band as shown in Fig.12.

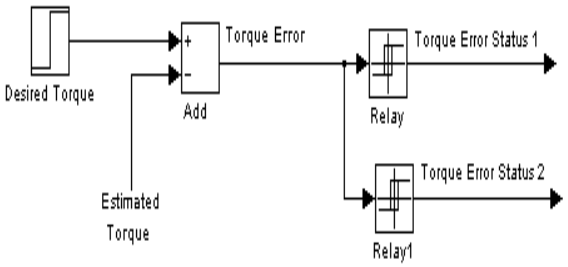

Fig.12. Design of torque controller.

In DTC, IM can operate in any of the four quadrant of the toque – speed plane as shown in Fig.13.

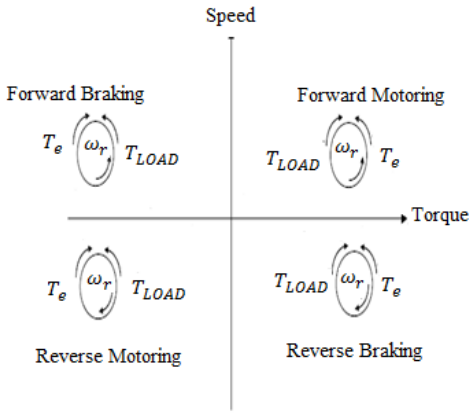

Fig.13. Four quadrant operation of IM.

X. VOLTAGE SOURCE INVERTER MODEL

In order to get the desired stator flux, the technique of space vector modulation is applied. To describe the concept of space vector modulation, Fig.14 shows a voltage source inverter (VSI) which is feeding a three phase induction motor. The inverter converts the DC to AC through power electronic devices such as an IGBT (Insulated bipolar gate transistor).

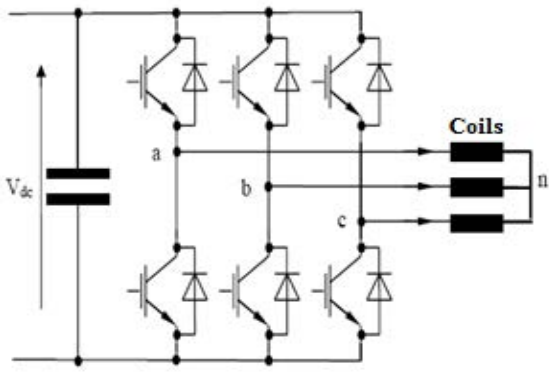

Fig.14. A voltage source inverter feeding three coils.

For simplicity, the stator resistor effect is neglected (i.e Rs = 0) and each of the three phase represents a coil where the three coils are STAR connected. The flux equation for each of the three leg can be expressed by the following formula [8].

$$\frac{d\vec{\psi}_s}{dt} = \vec{V}_s \qquad (23)$$

Alternatively, $\Delta\vec{\psi}_s = \vec{V}_s\,\Delta t$ (24)

$\vec{\psi}_s, \vec{V}_s$ are the stator flux and voltages respectively.

From (24), it can be noticed that the stator flux is proportional to the stator voltage. For clarification purposes, Fig.15 shows the possible states of VSI depending on the ON – OFF state of each IGBT.

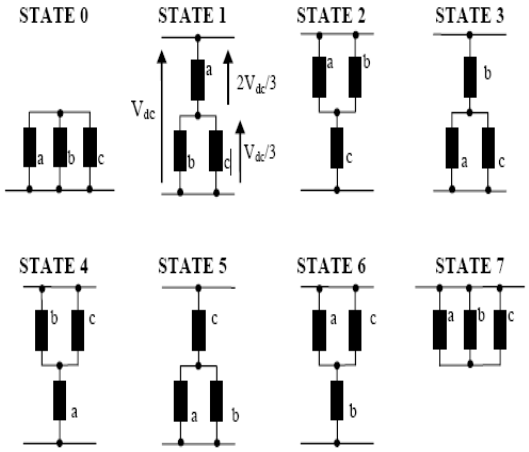

Fig .15. Switching states of three phase inverter .

There are eight states. However, two of them have null voltage and hence zero flux states. The remaining six states are illustrated in Fig.16.

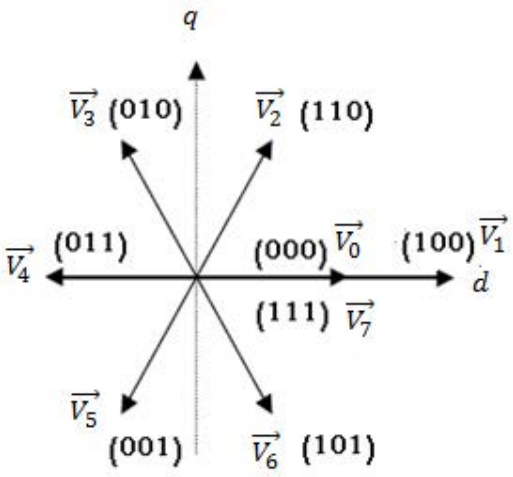

Fig.16. Inverter output voltage vectors.

The ON-state is indicated by number 1 while number zero indicates the off -state of the switching IGBT device. If $S_a, S_b$and S_c represent the combination of the switching devices conditions, it has been proved by [4] that the stator voltage is obtained by (25).

$$\overrightarrow{V_s} = \frac{2}{3} V_{dc} \left(S_a + e^{\frac{j2\pi}{3}} S_b + e^{\frac{j4\pi}{3}} S_c \right) \qquad (25)$$

By implementing this formula, a Simulink model for voltage source inverter has been designed as shown in Fig.17. The outputs of the inverter are the V_{ds} & V_{qs} which are plugged into the IM model.

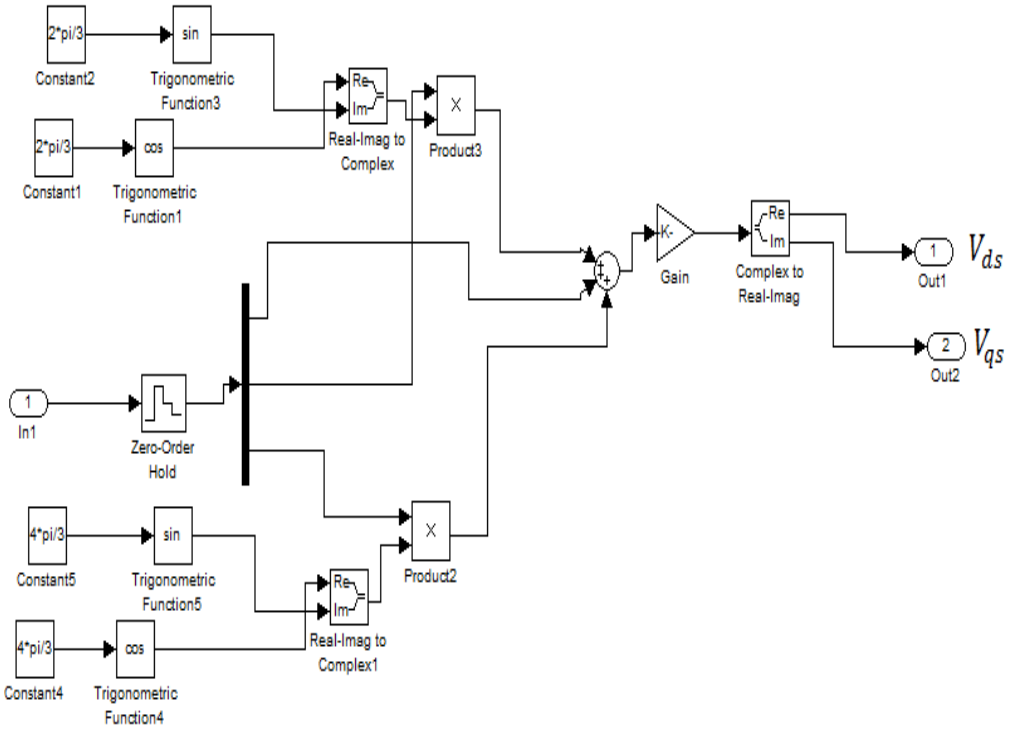

Fig.17. Design of voltage source inverter.

Considering the six sectors shown in Fig.22, the stator flux switching sectors can be distributed as follows.

$$-30^o < \theta_{s1} < 30^o$$
$$30^o < \theta_{s2} < 90^o$$
$$90^o < \theta_{s3} < 150^o$$
$$150^o < \theta_{s4} < 210^o$$
$$210^o < \theta_{s5} < 270^o$$
$$270^o < \theta_{s6} < 330^o$$

The stator flux angle in addition to the torque and flux hysteresis status are used to determine the suitable stator flux sector in order to apply the correct voltage vector to the induction motor operating under DTC. Table I lists the switching vectors in the different stator flux sectors.

Table I. Switching sectors of inverter voltage vectors

Error status of		Sector no.					
ψ_s	Te	1 θ_{s1}	2 θ_{s2}	3 θ_{s3}	4 θ_{s4}	5 θ_{s5}	6 θ_{s6}
0	1	110	010	011	001	101	100
	0	111	000	111	000	111	000
	-1	011	001	101	100	110	010
1	1	100	110	010	011	001	101
	0	000	111	000	111	000	111
	-1	001	101	100	110	010	011

A Simulink model has been built to implement the switching process as shown in Fig.18.

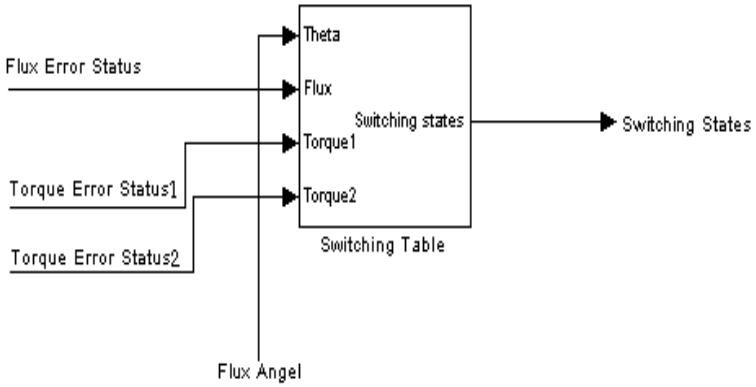

Fig.18. Switching Process model.

The individual Simulink models are connected together to form the complete model of the DTC shown in Fig .19.

XI. STUDY CASE

A 6 kW- 2 pole induction motor has been used to test the performance of the proposed model. The motor parameters are shown in Table II.

Table II. 6 KW IM parameters

Parameter	Value
R_s	1.19 Ω
R_r	1.04 Ω
L_s	0.01759 H
L_r	0.01759 H
L_m	0.55 H
Inertia, J	0.01 Kg*m²
No. of Poles	2
Applied voltage	415 V (line to line)
Frequency	50 Hz

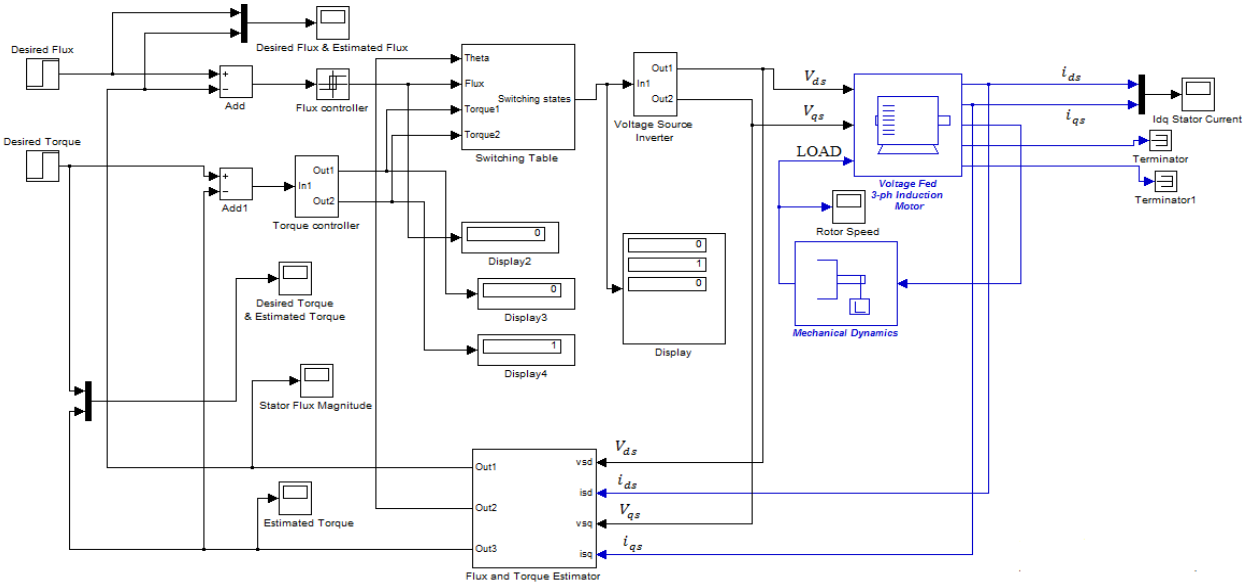

Fig.19. DTC Simulink model.

The speed-torque characteristic of the 6kW motor is shown in Fig.20.

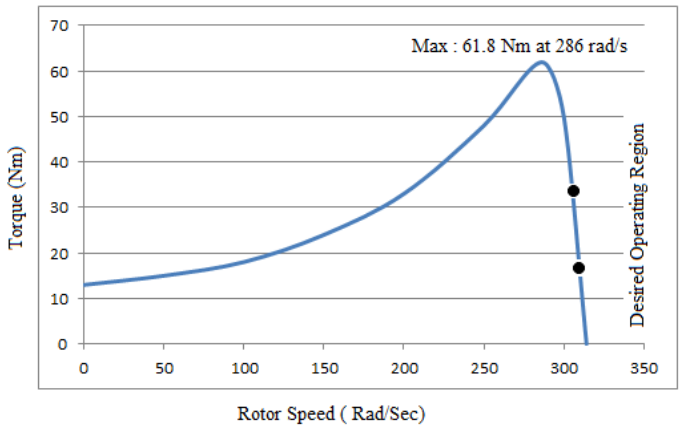

Fig.20. Speed-Torque Characteristic for the 6 kW IM.

By applying the equations mentioned in previous sections, the motor rated values are calculated and summarized in Table III. The motor is designed to run at 50Hz.

Table III. Data of the 6 kW IM

Quantity	Value
Synchronous Speed ω_s	314.2 $rads/sec$
Rotor Speed ω_r	307.5 $rads/sec$
Slip s	2.1 %
Stator Flux magnitude	1.28 Wb
Stator Flux Angle	280 degree
Torque	20.6 Nm

XII. SIMULATION RESULTS AND DISCUSSION

The DTC model has been tested at different mechanical loads.

A- No load

A step input of 20.6 Nm magnitude torque is applied after 0.05 sec. The torque and flux responses are shown in Fig.21.

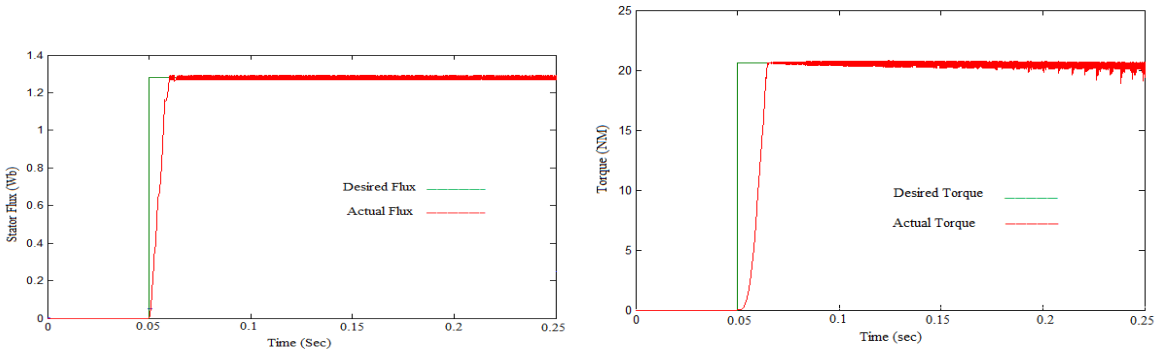

Fig.21. Flux and Torque responses at no load.

It can be noticed that there is no torque until the step input is applied at 0.05sec. Once the step input of 20.6 Nm is applied as the desired torque, the actual torque immediately increases in order to match with the target. Similarly, the stator flux goes up to catch the target of 1.28 Wb.

The hysteresis band is limited to ± 0.01 Wb and ± 0.01 Nm for flux and torque respectively. Fig.22 zooms in the flux and torque in order to show the hysteresis limits.

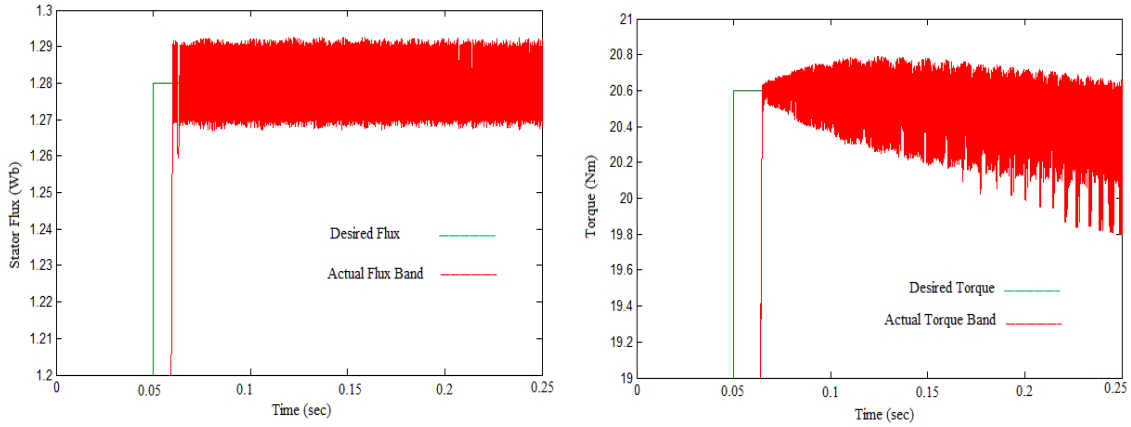

Fig.22. Band hysteresis of torque and flux.

Although the variation in the stator flux is quite small, it is enough to cause a significant starting up stator current as shown in Fig.23. To overcome this problem, a pre flux technique proposed by [9] may be applied so that the starting current is reduced and the motor and power converter devises are protected.

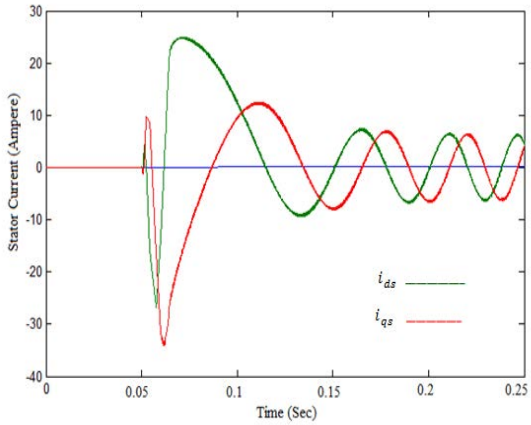

Fig.23. D-q axis stator currents.

B- 10Nm loads

Mechanical load of 10 *Nm* has been applied in order to test the transient performance of the developed DTC model. The flux is kept at required value as well as the torque. See Fig.24.

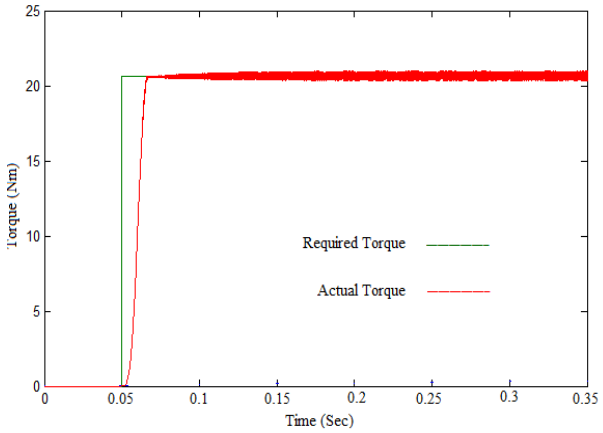

Fig.24. Torque at 10 *Nm* load.

C- 10 *Nm load at different torques*

A load torque step command is applied from +20 to -20 Nm in order to investigate the independence of torque and flux control. While the torque is changed at 0.22 sec in Fig.25, the flux stays the same. This confirms the main target of the DTC scheme which is to control the torque and flux separately.

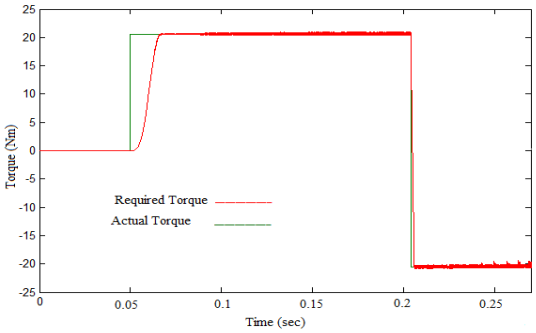

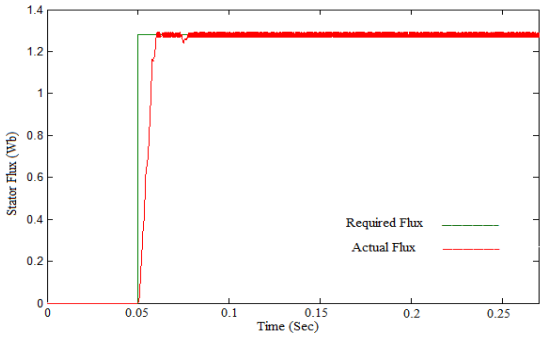

Fig.25. Torque and flux independence control.

The main observations of the simulation outcomes can be summarized as follows.

1- High accuracy of the DTC model has been proved for the stator flux. However, any small variation in the stator flux will cause a massive starting up stator current. This problem has also been observed by previous simulation [6].
2- Effectiveness of the DTC model has been demonstrated for the electromagnetic torque control with small inaccuracy.
3- The independent control of torque and stator flux has been confirmed for the proposed model.
4- Complexity in starting up current control and need of variable switching frequency as well as the need of flux and speed estimation are main drawbacks of the DTC scheme [10].

XIII. CONCLUSION

An induction motor model has been designed and its observability, controllability and stability have been shown. Then, Simulink sub-models have been designed for different components of DTC scheme. The proposed DTC model has been tested and evaluated on a 6kW induction machine. The outcomes of simulation have demonstrated a very high accuracy in flux and torque independent control. However, a significant starting up stator current is caused due to any small variation in the stator flux. Therefore, further work is required to limit the starting up stator current in order to protect the machine and power electronics devices.

REFERENCES

[1] Blaschke, F., “The principle of field orientation as applied to the new transvector closed loop system for rotating field machines”, Siemens Review, Vol.39, no.3, pp. 217 -220, May 1972.
[2] Marino, R., Tomei, P, and Verrelli, C., “Induction motor control design”, Textbook © Springer-Verlag London limited, 2010.
[3] B. K. Bose, “Modern Power Electronics and AC Drives”, Prentice- Hall, New Jersey, 2002.
[4] Abdul Wahab, H.F., and Sanusi, H., " Simulink Model of Direct Torque Control of Induction Machine", Amircan Journal of Applied Sciences, pp.1083 – 1090, 2008.
[5] Cruz,M. , Gallegos, A., Alvarez,R., and Pazos, F., “Comparsion of several nonlinear controllers for induction motor” ,in IEEE Int’l. Power Electronics Congress (CIEP), pp.134-139, 2004.
[6] Karlis, A.D., Kiriakopoulos, K., Papadopoulos, D.P., and Bibeau,E.L., " Comparison of the Field Oriented and Direct Torque Control Methods for Induction Motors used in Electric Vehicles", Democritus University of Thrace.
[7] I. Takahashi, T. Noguchi, “A new quick-response and high efficiency control strategy of an induction motor”, IEEE Trans. Ind. Appl., Vol. IA-22,No. 5, pp. 820-827, 1986.
[8] Esmaily, G., Khodabakhshian, A., and Jamshidi, K., “ Vector Control of Induction Motors Using UPWM Voltage Source Inverter ”, Isfahan University.
[9] Chapuis, Y.A. and D. Roye, “Direct torque control and current limitation method in start-up of an induction machine", IEE Conf. Power Electronics and Variable speed Drives, pp. 451 – 455, 1998.
[10] Silva, N.M., Martins, A.P., and Carvalho, A.S., “ Torque and Speed Modes Simulation of A DTC Controlled Induction Motor ”, Proceedings of the 10th IEEE Mediterranean Conference on Control Automation, MED'2002, Lisboa, pp. 1-6, July 2002.